A Distributed Model Predictive Control Strategy for Back-to-Back Converters

Luca Tarisciotti, *Member, IEEE*, Giovanni Lo Calzo, Alberto Gaeta, *Member, IEEE*, Pericle Zanchetta, *Senior Member, IEEE*, Felipe Valencia, *Member, IEEE* and Doris Saez, *Senior Member, IEEE*

***Abstract*— In recent years Model Predictive Control (MPC) has been successfully used for the control of power electronics converters with different topologies and for different applications. MPC offers many advantages over more traditional control techniques such as the ability to avoid cascaded control loops, easy inclusion of constraint and fast transient response. On the other hand, the controller computational burden increases exponentially with the system complexity and may result in an unfeasible realization on modern digital control boards. This paper proposes a novel Distributed Model Predictive Control, which is able to achieve the same performance of the classical Model Predictive Control whilst reducing the computational requirements of its implementation. The proposed control approach is tested on a AC/AC converter in a back-to-back configuration used for power flow management. Simulation results are provided and validated through experimental testing in several operating conditions.**

***Index Terms*—Predictive control, Nonlinear control systems, Back-to-back converters.**

I. Introduction

NOWADAYS power electronics is essential to all future sustainable energy scenarios since it is the only technology that can deliver efficient and flexible conversion and conditioning of electrical energy. It is vital in many low carbon applications including renewable energy generation, smart grids, electric transport (Electric Vehicles, Hybrid Electric Vehicles, rail), aerospace, energy saving, motor drives and lighting. During the past few decades there has been a proliferation of converter topologies and technical solutions for various applications both in scientific literature and in Industry. Traditional linear control approaches have been widely used for power converters; however many other control strategies have been proposed in literature and successfully tested, among which Model Predictive Control.

MPC is an optimal control technique whose objective is to regulate the states and/or the outputs of the system towards their desired values. This is achieved minimizing a cost function inside a feasible region [1], [2]. That is, MPC computes optimal control inputs so that physical and operational constraints of the system to be controlled are fulfilled. Due to its ability to handle complex systems with input and state constraints, MPC is becoming one of the most successful advanced control techniques implemented in industry [3]–[5]. For controlling power-electronics-based devices, several MPC approaches have been proposed in the specialized literature [6]–[13]. In [6], [7], [10] a complete review of those techniques is presented. From that review, the authors concluded that one of the mayor challenges for MPC schemes for power converters is to ensure that the computational burden of the optimization problem allow obtaining solutions within a reasonable sampling time, especially when the prediction horizon is greater than one sampling interval, or when the number of switching states increases. Regarding the length of the prediction horizon, in [11] a literature review of MPC approaches with prediction horizon larger than one is reported and examples of their applicability are presented. As for the increasing number of converter switching states, above all in novel topologies, some finite-control-set MPC (FCS-MPC) approaches as well as generalized predictive control (GPC) were posed as alternatives in [10]. In particular, FCS-MPC was successfully implemented by using a reduced set of switching states as in [6], [7], [9], [14], [15]. In [16]–[21] FCS-MPC implementations were used for converters with a higher number of switching states, such as Cascaded H-Bridge and Diode Clamped converters. However, if the number of states increases further, the implementation of these FCS-MPC strategies may become unfeasible. Moreover, when using FCS-MPC, the converter switching frequency is always lower than half of the sampling frequency; therefore a high sampling frequency is usually preferred, thus reducing the available computational time on modern DSP based control boards. Indeed, one of the main conclusions obtained in [10], [11] was that finding computationally efficient FCS-MPC control algorithms for power converters is still an open issue.

Motivated by the good performance of the FCS-MPC in different reported applications, in this paper an alternative formulation for this control problem is proposed, named Distributed Model Predictive Control (DMPC) [1], [5], [22]–[28]. Specifically, the FCS-MPC problem is formulated in a distributed fashion, reducing the computational time and allowing its implementation in complex power converters, such as back-to-back converters and multi-level converters. In the proposed approach the entire system is divided into simpler subsystems. For each subsystem an FCS-MPC is formulated. The single controllers are able to communicate with each other in order to jointly decide the local switching sequence. The proposed FCS-MPC formulation is able to provide a feasible control implementation for systems with hard requirements involving fault tolerance, flexibility, and high control capabilities, without the solution of one large centralized optimization problem [29]–[31]. DMPC has been applied to power control of wind turbines [32], [33], voltage control of microgrids [34]–[36] and sequential or iterative control of industrial processes [37]–[40]. However it has rarely been

Manuscript received June 15, 2015; revised November 13, 2015; accepted January 13, 2016.

applied to the low-level control of a power electronic converter. In order to prove DMPC feasibility for the latter case, in this work a Back-to-Back converter topology is used to implement and test the performance of DMPC, by both simulation and experimental tests.

The paper is organized as follows: Section II presents the DMPC framework as well as its application to the control of a Back-to-Back converter. Section III presents the simulations results whereas Section IV depicts the experimental results obtained with a Back-to-Back converter. In Section V the concluding remarks are put forward.

II. Distributed Model Predicted Control

In Fig. 1 the DMPC scheme is shown for the case of two subsystems. In this figure, Process 1 and Process 2 have local MPC controllers. Since these processes interact with each other, sharing information between controllers is required in order to allow them to compute their own control actions. Otherwise, the system may lose performance and/or stability. In order to avoid that, at each time step local controllers must decide about the control actions to be locally applied and transmit them to the other controllers. In [26], [41]–[43] several DMPC approaches are discussed. Moreover, in [1], [5], [22]–[28], [30], [43], [44] some specific DMPC schemes are presented. Almost all of them have been applied to systems with sampling times in the range between seconds and minutes. The aim of this section is to present the DMPC as an alternative for controlling systems whose dynamics are in the microseconds range, particularly as an alternative for optimally controlling power converters.

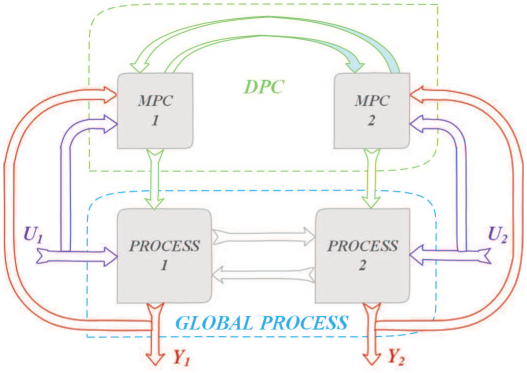

Fig. 1: Schematic diagram of a typical DMPC scheme.

A. Mathematical Formulation of the DMPC Problem

Consider the discrete-time non-linear system

$$\begin{aligned} x(k+1) &= f(x(k),u(k)) \\ y(k) &= g(x(k),u(k)) \end{aligned} \tag{1}$$

where $x(k)$, $u(k)$, and $y(k)$ respectively denote the state, input, and output vectors of the dynamical system at time instant k, with $f(x(k),u(k))$ and $g(x(k),u(k))$ non-linear functions describing the time evolution of the system to be controlled. The idea behind MPC is to compute a sequence of control actions $\tilde{u}(k) = \left[u^T(k+1),\ldots,u^T(k+N_p-1)\right]^T$ such that a cost function is minimized throughout a prediction horizon N_p. With this purpose, the system model (1) is used to estimate the behavior of the controlled system and the quadratic cost function (2) is used to measure its performance, where $e(h+1/k) = y_{ref}(h+1) - y(h+1/k)$ is the difference between the desired and the predicted output, $y_{ref}(h+1)$ being the desired system output and $y(h+1/k)$ being the predicted system output at time step $h+1$ given the measured state values at time step k; and Q and R are positive definite weighting matrices, very often diagonal.

$$\begin{aligned} L(\tilde{x}(k),\tilde{u}(k)) = &\sum_{h=k}^{k+N_p-1}\left[e^T(h+1/k)Qe(h+1/k)\right] \\ &+ \sum_{h=k}^{k+N_p-1}\left[u^T(h)Ru(h)\right] \end{aligned} \tag{2}$$

Although MPC has broadly recognized advantages over single-input single-output and even over other multiple-input multiple-output control strategies, its main disadvantage is the computational burden associated with its implementation. Thereby, as the number of inputs increase its implementation becomes hardly feasible. Furthermore, if the sampling time decreases (as in the case of power electronic devises) its implementation becomes hardly feasible as well. In both cases, an alternative for coping with these shortcomings is implementing MPC in a distributed fashion.

Assume that the whole system (1) can be decomposed into M subsystems

$$\begin{aligned} x_r(k+1) &= f_r(x(k),u_r(k),u_{-r}(k)) \\ y_r(k) &= g_r(x(k),u_r(k),u_{-r}(k)) \end{aligned} \tag{3}$$

where, $x_r(k)$, $u_r(k)$, and $y_r(k)$ are the local states, inputs, and outputs of subsystem r, and $u_{-r}(k)$ is a vector containing all control inputs but the local $u_r(k)$; that is

$$u_{-r}(k) = [u_1^T(k),\ldots,u_{r-1}^T(k),u_{r+1}^T(k),\ldots,u_M^T(k)]^T \tag{4}$$

As in the case of MPC, the idea behind DMPC is to compute the control actions to be locally applied to the system $\tilde{u}_r(k) = \left[u_r^T(h+1),\ldots,u_r^T(h+N_p-1)\right]^T$ given the behavior predicted by using the local system model (3), so that both global and local cost functions are minimized. For the r-th local controller, let $e_r(h+1/k) = y_{ref\_r}(h+1) - y_r(h+1/k)$ denote the difference between the desired and the predicted local output at time step $h+1$ given the measured state values at time step k, where $y_{ref\_r}(h+1)$ denotes the desired output and $y_r(h+1/k)$ denotes the predicted output. Let Q_r and R_r be the local weighting matrices, i.e., diagonal matrices of proper dimension with positive elements. Then replacing local models into the global cost function (2) yields

$$L(\tilde{x}(k),\tilde{u}(k)) = \sum_{r=1}^{M}\left[\sum_{h=k}^{k+N_p-1}\left[e_r^T(h+1/k)Q_r e_r(h+1/k)\right] + \sum_{h=k}^{k+N_p-1}\left[u_r^T(h)R_r u_r(h)\right]\right] \quad (5)$$

Let $L_r(\tilde{x}(k),\tilde{u}_r(k),\tilde{u}_{-r}(k))$ denote the cost function for the local controller *r*. From equation (5), it is defined as

$$L_r(\tilde{x}(k),\tilde{u}_r(k),\tilde{u}_{-r}(k)) = \sum_{h=k}^{k+N_p-1}\left[e_r^T(h+1/k)Q_r e_r(h+1/k)\right] + \sum_{h=k}^{k+N_p-1}\left[u_r^T(h)R_r u_r(h)\right] \quad (6)$$

Thus, $L(\tilde{x}(k),\tilde{u}(k)) = \sum_{r=1}^{M} L_r(\tilde{x}(k),\tilde{u}_r(k),\tilde{u}_{-r}(k))$, where, for the local controller *r*, $\tilde{u}_r(k) = [u_r^T(h+1),\ldots,u_r^T(h+N_p-1)]^T$ denotes the sequence of optimal local control actions at time step *k*, and $\tilde{u}_{-r}(k) = [\tilde{u}_1^T(k),\ldots,\tilde{u}_{r-1}^T(k),\tilde{u}_{r+1}^T(k),\ldots,\tilde{u}_M^T(k)]^T$ denotes the sequences of control actions of the remaining controllers. In this paper, those sequences are assumed constant and equal to their measured value throughout N_p. It is important to remark that the performance of each controller depends upon the decisions made by the remaining controllers. Specifically, for controller *r* both local cost function and predictions of the output are function of the measured state and input values by the remaining controllers. Hence, it is not enough to find the sequence $\tilde{u}_r(k)$ but also to quantify its impact in the performance of the remainder controllers. With this purpose, instead of minimizing $L_r(\tilde{x}(k),\tilde{u}_r(k),\tilde{u}_{-r}(k))$, each controller *r* minimize $L(\tilde{x}(k),\tilde{u}(k))$ with respect to its own local variables. Then, each local MPC is formulated as

$$\begin{aligned} &\min_{\tilde{u}_r(k)} \sum_{r=1}^{M} L_r(\tilde{x}(k),\tilde{u}_r(k),\tilde{u}_{-r}(k)) \\ &\text{s.t.:} \\ &x_r(h+1/k) = f_r(x(h/k),u_r(h),u_{-r}(h)) \\ &y_r(h) = g_r(x(h/k),u_r(h),u_{-r}(h)) \end{aligned} \quad (7)$$

Note that minimization problem (7) only included the constraints associated with the dynamic behavior of the system to be controlled. However, other constraints could be also added. These constraints often are defined by maximum and minimum allowed values for the states, inputs, and/or outputs. Therefore, in the general case the constraints of (7) are given by $x_r(h) \in \mathbf{X}_r(x(k),u_r(k),u_{-r}(k))$, for the trajectories of the local states, $u_r(h) \in \mathbf{U}_r(x(k),u_r(k),u_{-r}(k))$ for the local inputs, and $y_r(h) \in \mathbf{Y}_r(x(k),u_r(k),u_{-r}(k))$ for the local outputs, where $\mathbf{X}_r(x(k),u_r(k),u_{-r}(k))$, $\mathbf{U}_r(x(k),u_r(k),u_{-r}(k))$, and $\mathbf{Y}_r(x(k),u_r(k),u_{-r}(k))$ are the feasible sets for the local states, the local inputs, and the local outputs respectively.

The minimization problem (7) extends the DMPC proposed in [1] to systems in which a non-linear prediction model and the coupling among the constraints is considered. Nevertheless, the main contribution of this paper is the application of the DMPC to the control of power converters. To reduce the computational burden deriving from its solution, in the proposed DMPC the controller *r* computes its optimal sequence of control actions $\tilde{u}_r(k)$ assuming the remaining sequences of control actions $\tilde{u}_{-r}(k)$ constant and equal to their current measured values. Then, each controller sends to the remaining controllers the control actions that it is currently being applied. Furthermore, each controller measures its local states and sends those measurements to the remainder controllers so that each controller has the state vector $x(k)$. With the local measurements, and the information received from the other controllers, controller *r* is able to estimate the feasible sets $\mathbf{X}_r(x(k),u_r(k),u_{-r}(k))$, $\mathbf{U}_r(x(k),u_r(k),u_{-r}(k))$, and $\mathbf{Y}_r(x(k),u_r(k),u_{-r}(k))$, and also is able to solve (7). The following steps are necessary for implementing the proposed distributed control strategy:

1. Each subsystem measures and sends to the remaining subsystems the values of its corresponding states $x_r(k)$ and control inputs $u_r(k)$.
2. With the information provided by the remainder of them, each subsystem solves the minimization problem in (10).
3. Each subsystem updates its control action sequence as $u_r(k+1) = u_r^*(k)$, with $u_r^*(k)$ being the optimal solution of (10).
4. The first element of the sequence is applied and the remaining elements are used as the initial conditions for the next time step.

In comparison with the algorithm in [18], the steps suggested in this paper do not involve iterative procedures to obtain $\tilde{u}_r(k)$. Furthermore, contrary to the procedure in [18], both subsystems weighting and the update of $\tilde{u}_r(k)$ according to the weight assigned to each subsystem are prevented. Consequently, the complexity and the computational burden of the DMPC are both reduced. This is particularly important when DMPC is applied to power electronics converter control. In fact, these systems can became rather complex and present a broad control set that is hard to compute even using fast DSP control boards. For example in case of multilevel converters, the control set can include several hundreds of converter states [45]–[48] and, thus, a centralized MPC implementation became hardly feasible.

However, when (10) is proposed for power converters control, in the specialized literature several other approaches for non-linear DMPC have been reported [34].

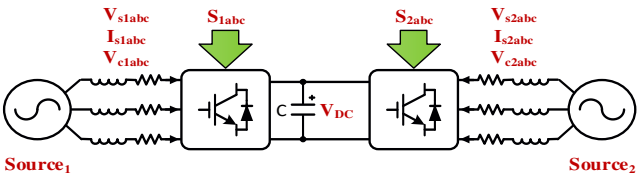

Fig. 2: Schematic view of the setup used to formulate the proposed DMPC strategy.

B. Back-to-Back Converter Application

The proposed DMPC is applied to the direct power control and DC-Link voltage control of a Back-to-Back converter, shown in Fig.2.The Back-To-Back configuration considered in this work, allows the power transfer (both active and reactive) between the two energy sources (or grids) V_{s1abc} and V_{s2abc} while keeping the capacitor voltage V_{DC} regulated at a desired value. With this aim, the switching states $S_{1abc}(t)$ and $S_{2abc}(t)$ are computed within each sampling interval, usually in the order of tens of microseconds [9], [18], [49], [50]. The two power converters considered here are traditional three-phase two level structures in order to simplify the system configuration and demonstrate the feasibility of the proposed control approach. However more complex topologies could be considered, like multilevel converters, for example in high power applications. In

Fig. 2, the variables I_{s1abc}, I_{s2abc}, V_{c1abc} and V_{c2abc} respectively denote the measured currents and voltages at grids 1 and 2. Furthermore, series *L-R* filters L_1-r_{L1} and L_2-r_{L2} were considered as commonly found in grid connected power converters (e.g. photovoltaic inverters or active front ends for drives). This system is described from the following set of equations, where $k_1=T_s/L_1$, $k_2= r_{L1}T_s/L_1$, $k_3=T_s/L_3$, $k_4= r_{L2}T_s/L_2$, $k_5=T_s/C$.

$$\begin{aligned} I_{s1abc}(h+1) &= I_{s1abc}(h)+k_1\left(V_{s1abc}(h)-V_{DC}(h)S_{1abc}(h)\right)-k_2 I_{s1abc}(h)\\ I_{s2abc}(h+1) &= I_{s2abc}(h)+k_3\left(V_{s2abc}(h)-V_{DC}(h)S_{2abc}(h)\right)-k_4 I_{s2abc}(h)\\ V_{DC}(h+1) &= V_{DC}(h)+k_5\left(I^T_{s1abc}(h)S_{1abc}(h)-I^T_{s2abc}S_{2abc}(h)\right) \end{aligned} \tag{8}$$

This model is converted from the natural reference frame (e.g. *abc*) in a stationary reference frame (e.g. $\alpha\beta$) using the Clarke's transform. The final model used for the control design is shown in the following set of equations.

$$\begin{aligned} I_{s1\alpha\beta}(h+1) &= I_{s1\alpha\beta}(h)+k_1\left(V_{s1\alpha\beta}(h)-V_{DC}(h)S_{1\alpha\beta}(h)\right)-k_2 I_{s1\alpha\beta}(h)\\ I_{s2\alpha\beta}(h+1) &= I_{s2\alpha\beta}(h)+k_3\left(V_{s2\alpha\beta}(h)-V_{DC}(h)S_{2\alpha\beta}(h)\right)-k_4 I_{s2\alpha\beta}(h)\\ V_{DC}(h+1) &= V_{DC}(h)+k_5\left(I^T_{s1\alpha\beta}(h)S_{1\alpha\beta}(h)-I^T_{s2\alpha\beta}(h)S_{2\alpha\beta}(h)\right) \end{aligned} \tag{9}$$

When MPC is applied to such system if a finite control set is considered 8 switching states for each converter side can be applied. Thus, the classical FCS-MPC for this converter needs to evaluate all the possible combination of switching states (8^2=64). When using DMPC it is possible to separate the control problem in two subsystems, each of them having its own FCS-MPC controller and thus reducing the number of switching states combination to evaluate to 8×2=16. This data shows that using DMPC the controller computational burden is approximately one fourth of classical FCS-MPC. However communication between the controller algorithms of the two converter sides are needed in order to maintain the DC-Link well regulated.

In order to formulate the DMPC control problem, let $x(h)=\left[I^T_{s1\alpha\beta}(h), I^T_{s2\alpha\beta}(h), V_{DC}(h)\right]^T$ be the state vector of the system. Then, with the proposed partitioning, and given the framework presented in Section II-A (specifically equations (5)-(7)), the following local cost functions are defined for the control of the back-to-back converter:

$$\begin{aligned} L_1(\tilde{x}(k),\tilde{S}_{1\alpha\beta}(k),\tilde{S}_{2\alpha\beta}(k)) &= e_1^T(k+1/k)\tilde{Q}_1 e_1(2/k)\\ L_2(\tilde{x}(k),\tilde{S}_{\alpha\beta1}(k),\tilde{S}_{\alpha\beta2}(k)) &= e_2^T(k+1/k)\tilde{Q}_2 e_2(2/k) \end{aligned} \tag{10}$$

with

$$e_1(k+1/k)=\left[P_{1ref}-P_1(k+1/k), Q_{1ref}-Q_1(k+1/k), V_{DCref}-V_{DC}(k+1/k)\right]^T \tag{11}$$

$$e_2(k+1/k)=\left[P_{2ref}-P_2(k+1/k), Q_{2ref}-Q_2(k+1/k), V_{DCref}-V_{DC}(k+1/k)\right]^T \tag{12}$$

and $\tilde{Q}_1\in\mathbf{R}^{3\times3}$, $\tilde{Q}_2\in\mathbf{R}^{3\times3}$ diagonal matrices with positive elements. Note that the local cost functions $L_1(\tilde{x}(k),\tilde{S}_{1\alpha\beta}(k),\tilde{S}_{2\alpha\beta}(k))$ and $L_2(\tilde{x}(k),\tilde{S}_{1\alpha\beta}(k),\tilde{S}_{2\alpha\beta}(k))$ are only coupled by the deviation of the capacitor voltage. Indeed, according to the converter model (9), this is the only term that is affected by both subsystems.

With the local cost functions $L_1(\tilde{x}(k),\tilde{S}_{1\alpha\beta}(k),\tilde{S}_{2\alpha\beta}(k))$ and $L_2(\tilde{x}(k),\tilde{S}_{1\alpha\beta}(k),\tilde{S}_{2\alpha\beta}(k))$ already defined, the sequence $\tilde{S}_{1\alpha\beta}(k)$ is given by the solution of the following optimization problem:

$$\begin{aligned} &\min_{\tilde{S}_{1\alpha\beta}(k)} L_1(\tilde{x}(k),\tilde{S}_{1\alpha\beta}(k),\tilde{S}_{2\alpha\beta}(k))+L_2(\tilde{x}(k),\tilde{S}_{1\alpha\beta}(k),\tilde{S}_{2\alpha\beta}(k))\\ &\text{s.t.:}\\ &x_1(h)\in\mathbf{X}_1(x(k),S_{1\alpha\beta}(h),S_{2\alpha\beta}(h))\\ &S_{1\alpha\beta}(h)\in\mathbf{U}_1(x(k),S_{1\alpha\beta}(h),S_{2\alpha\beta}(h))\\ &P_1(h)\in\mathbf{Y}_{P1}(x(k),S_{1\alpha\beta}(h),S_{2\alpha\beta}(h))\\ &Q_1(h)\in\mathbf{Y}_{Q1}(x(k),S_{1\alpha\beta}(h),S_{2\alpha\beta}(h)) \end{aligned} \tag{13}$$

whereas the sequence $\tilde{S}_{2\alpha\beta}(k)$ is obtained by solving the minimization problem

$$\begin{aligned} &\min_{\tilde{S}_{2\alpha\beta}(k)} L_1(\tilde{x}(k),\tilde{S}_{1\alpha\beta}(k),\tilde{S}_{2\alpha\beta}(k))+L_2\left(\tilde{x}(k),\tilde{S}_{1\alpha\beta}(k),\tilde{S}_{2\alpha\beta}(k)\right)\\ &\text{s.t.:}\\ &x_2(h)\in\mathbf{X}_2\left(x(h),S_{1\alpha\beta}(h),S_{2\alpha\beta}(h)\right)\\ &S_{2\alpha\beta}(h)\in\mathbf{U}_2\left(x(h),S_{1\alpha\beta}(h),S_{2\alpha\beta}(h)\right)\\ &P_2(h)\in\mathbf{Y}_{P2}\left(x(h),S_{1\alpha\beta}(h),S_{2\alpha\beta}(h)\right)\\ &Q_2(h)\in\mathbf{Y}_{Q2}\left(x(h),S_{1\alpha\beta}(h),S_{2\alpha\beta}(h)\right) \end{aligned} \tag{14}$$

where $\mathbf{Y}_{P1}\left(x(h),S_{1\alpha\beta}(h),S_{2\alpha\beta}(h)\right)$, $\mathbf{Y}_{P2}\left(x(h),S_{1\alpha\beta}(h),S_{2\alpha\beta}(h)\right)$, and $\mathbf{Y}_{Q1}\left(x(h),S_{1\alpha\beta}(h),S_{2\alpha\beta}(h)\right)$, $\mathbf{Y}_{Q2}\left(x(h),S_{1\alpha\beta}(h),S_{2\alpha\beta}(h)\right)$ are the control sets for the active and reactive power at each side of the converter.

In order to implement this control strategy, the active power references must be calculated. Given the desired value for the voltage at the capacitor, V_{DCref}, and given the actual measured voltage value, V_{DC}, the required change in the active power flow to regulate the voltage at the desired value is given by

$$P_{DC}=\frac{C}{2NT_s}\left(V^2_{DCref}-V^2_{DC}\right) \tag{15}$$

where N denotes the desired number of time steps required for reaching the desired value, and C is the capacitance of the DC link. Once the value of P_{DC} is computed, the desired active power transfer should be modified accordingly. In this case,

such a variation was equally distributed between the two converter sides, i.e., $P_{1\text{ref}} = P_{1\text{des}} + 0.5P_{\text{DC}}$ and $P_{2\text{ref}} = P_{2\text{des}} + 0.5P_{\text{DC}}$, with $P_{1\text{des}}$ and $P_{2\text{des}}$ the desired power transfer from one side of the converter to the other. It is important to highlight that, since the active power balance through the converter has always to be equal to 0, P_{1des} and P_{2des} have to be chosen with the same value but opposite sign. Additionally, exploiting the α-β model of the converter, the active and reactive power flow through the converter is predicted as follows:

$$\begin{aligned} P_i(h) &= \frac{3}{2}\left(V_{si\alpha}(h)I_{si\alpha}(h) + V_{si\beta}(h)I_{si\beta}(h)\right) \\ Q_i(h) &= \frac{3}{2}\left(V_{si\beta}(h)I_{si\alpha}(h) - V_{si\alpha}(h)I_{si\beta}(h)\right) \end{aligned} \quad i = 1,2 \quad (16)$$

Note that the prediction of the active and reactive power as well as the prediction of the source currents requires the knowledge of the source voltage evolution at both sides. Thus, given the current and the past voltage a measurement, the voltage at the next time step is computed using a first order Lagrange extrapolation:

$$\begin{aligned} V_{si\alpha}(h+1) &= 2V_{si\alpha}(h) - V_{si\alpha}(h-1) \\ V_{si\beta}(h+1) &= 2V_{si\beta}(h) - V_{si\beta}(h-1) \end{aligned} \quad i = 1,2 \quad (17)$$

Even if the prediction horizon N_p has been set to 1 in this DMPC application, a two-step ahead prediction is required, in order to take into account the one sampling interval delay introduced by the digital implementation. In fact the first step of prediction is related only to the measured variables and the switching states calculated during the previous sampling interval. Then, taking these predicted values as initial conditions, the values of $\tilde{S}_{1\alpha\beta}(k)$ and $\tilde{S}_{2\alpha\beta}(k)$ are computed according to (13) and (14). However, due to the reduction of the time required for computing $\tilde{S}_{1\alpha\beta}(k)$ and $\tilde{S}_{2\alpha\beta}(k)$, prediction horizons longer than 1 could be implemented using the proposed DMPC.

Fig 3 shows the detailed block schemes of the implemented DMPC for a Back-To-Back converter and the coupling between the two converters control can be appreciated. The control of each converter side has to be executed 8 times in order to calculate the minimum cost function value. This represents a consistent reduction of the number of iteration, when compared with classical MPC which has to be executed 64 times before reaching the minimum cost function value. For each side of the converter the following implementation step has to be sequentially executed:

1. Calculate the Active power reference according to (16).
2. Calculate the state variables (AC currents and DC-Link voltage) prediction using (9). It is important to note that, since the control is distributed, the control of side 1 uses the output of the controller on side 2 (i.e. the side 2 converter state) to calculate the DC-link voltage prediction and vice versa on converter side 2.
3. Calculate Active and Reactive power predictions using (16) and (17).
4. Calculate the cost functions in (10).
5. Repeat the steps 1-4 for the 8 possible converter states on each converter side.
6. Identify the minimum cost function value on each side and select the switches state on each converter side accordingly.

III. Simulation Results

The proposed DMPC has been at first tested and compared with centralized FCS-MPC using a MATLAB-PLECS co-simulation. As it will be shown, DMPC is able to maintain the same performances of the classical FCS-MPC. For such reason and considering that FCS-MPC has been widely described and compared in literature, comparison with other control techniques has been avoided. The parameters for the simulated system, reflecting the experimental setup of Fig. 4, are listed in Table I. Using the setup of Fig.4 the system does not need any resistive load since the power is able to circulate through both converter sides while the voltage source provides only the system losses. Step changes in active and reactive power flows between port 1 and 2 with maximum values of respectively 4kW and 1kVAR are shown in Fig. 5. The reference values are accurately followed while the variation of the DC-Link voltage remains limited. It should be noted that initially, although all the reference powers are set to zero, a small amount of power is drained from both grids to maintain the DC-Link voltage at the desired level, as a consequence of the presence of discharge resistors in parallel with the DC-Link capacitors.

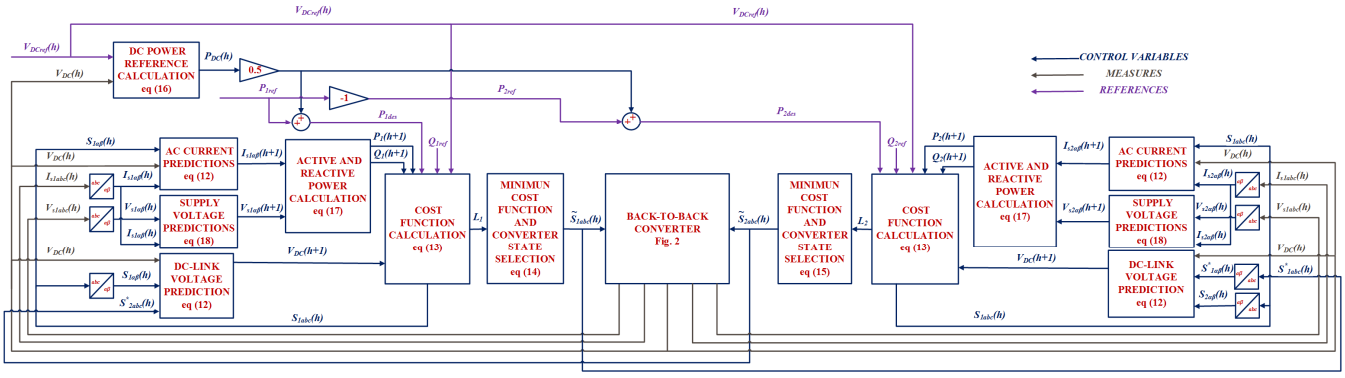

Fig.3 Detailed block scheme of the implemented DMPC for a Back-To-Back converter.

TABLE I: SYSTEM PARAMETERS

Symbol	Description	Value [a]
L_1, L_2	Line inductances	11 [mH]
r_{L1}, r_{L2}	DC resistance of line inductors	200 [mΩ]
C	DC-Link capacitance	3.6 [mF]
T_s	Sampling time	100μs
V_{s1abc}	Grid 1 RMS phase voltage	180Vrms
V_{s2abc}	Grid 2 RMS phase voltage	60Vrms
F	Grids Frequency	50Hz
N	DC-Link voltage horizon	100
w_1	Cost Function weight for active and reactive power	1
w_2	Cost Function weight for the DC-Link voltage	20

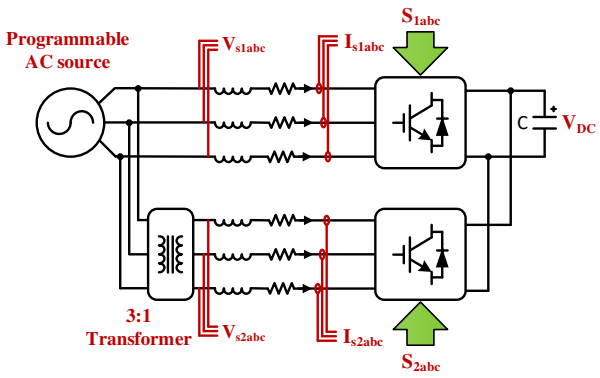

Fig. 4: Experimental setup used for validating the proposed DMPC strategy.

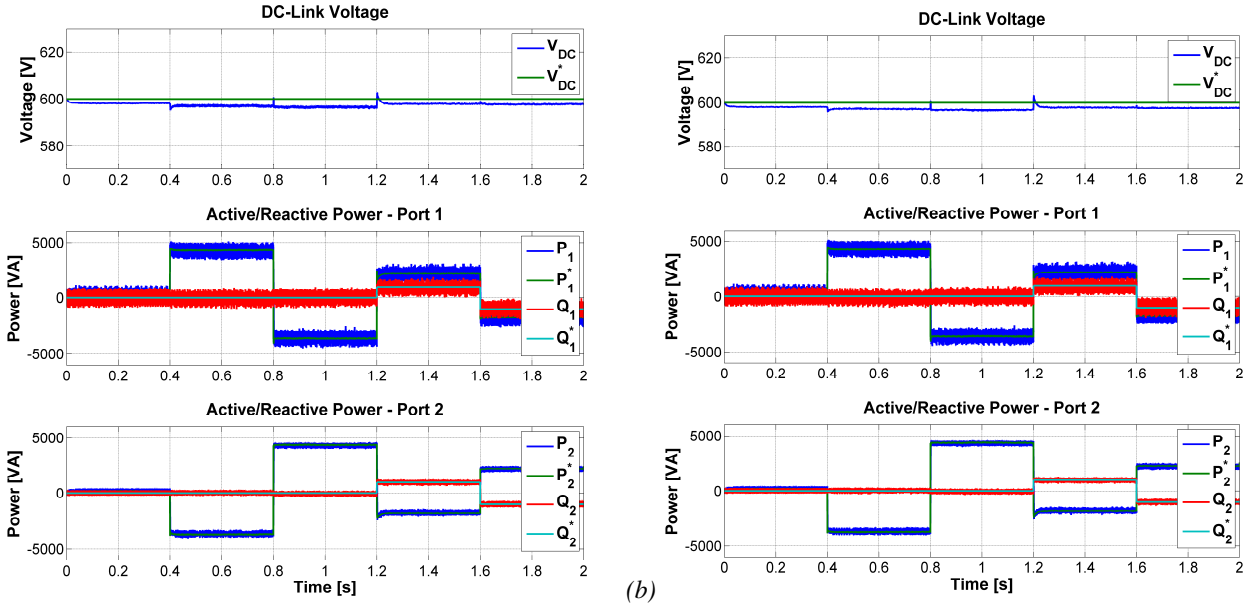

Fig. 5: Simulation results – Step changes in the demanded active (blue) and reactive (red) power flows. From top to bottom: reference and measured DC-Link voltages, reference and measured powers at port 1, reference and measured powers at port 2: (a) MPC (b) DPC.

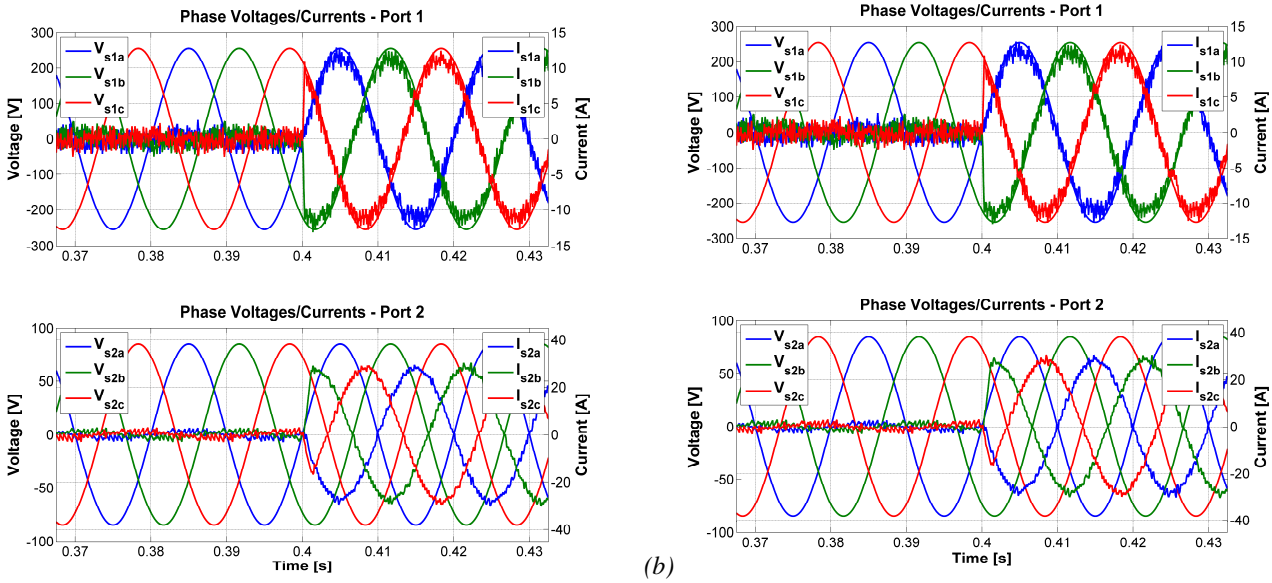

Fig. 6: Simulation results - Measured phase voltages and currents at port 1 (up) and port 2 (bottom) before and after a 4 KW change in the demanded active power: (a) MPC (b) DPC.

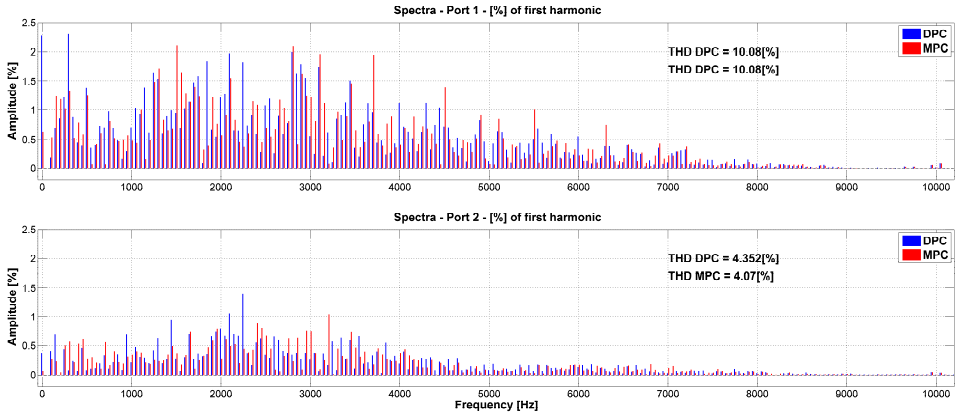

Fig. 7: Simulation results - Frequency spectrum of the measured phase currents at port 1 (up) and port 2 (bottom)

Measured phase voltages and currents before and after the demanded active power step at t=0.4s of Fig. 5 are shown in Fig. 6. In this particular case 4KW are drained from grid 1 and fed into grid 2. As it can be noted a fast current transient, without noticeable overshoot is achieved. The frequency spectrum for the phase currents when providing 4kW of active power and 0kVAR of reactive power are shown in Fig. 7. As expected since DMPC, as FCS-MPC, has a variable switching frequency lower than the sampling frequency, low order harmonics can be noted. However, the magnitude of the various harmonics remains below 3%. Overall, MPC and DPC achieve the same transient performance while the steady state performance of DPC are marginally deteriorated, with respect of MPC, by the delay introduced between the two partitions of the distributed control technique.

IV. Experimental Results

Experimental tests have been carried out on the 20kW Back-To-Back converter of Fig. 7. A programmable AC source has been used for emulating the grid under ideal and non-ideal operating conditions, such as grid voltage dips and frequency changes. A 3:1 transformer has been inserted between the AC source and one of the two inverters as shown in Fig. 4 in order to demonstrate the feasibility of the proposed control strategy even when the Back-to-Back converter operates as solid-state transformer between grids at different voltages.

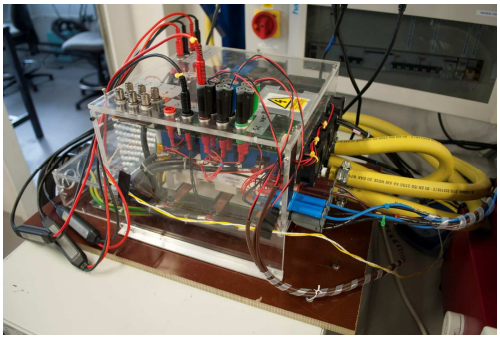

Fig. 8- Back-to-Back converter used during experimental testing.

Due to the high power rating of the IGBT modules used in this converter (1.2 kV, 400 A) and due to their consequent impossibility to work at switching frequencies higher than few kHz, the sampling period for the control has been set to 100 µs as listed in Table I.. However, the use of modern Silicon Carbide devices, not available on the converter used for the experimental tests, allows obtaining a higher switching frequency for the same power rating of the application. Given the variable switching frequency of DMPC (typically around half of the sampling frequency) and the difficulty to use a lower sampling time in the available experimental rig, has resulted in increased values of the L-R filters and DC-Link parameters. The control board (not shown in Fig. 7 and connected to the converter using fiber optic cables) used during the experimental testing feature a Texas Instruments C6713 DSP together with a ProAsic 3 FPGA. The executions time on this control platform are calculated and shown in Fig. 8 where it is clear that, without considering the time necessary for executing communication protocols, The execution time for DMPC is 50% smaller of the FCS-MPC execution time. This allows DMPC to be implemented at much higher sampling frequencies than classical FCS-MPC, while a sampling frequency of 10kHz is already critical for the implementation of a classical FCS-MPC, which takes the 89% of the available time (100µs) to be executed.

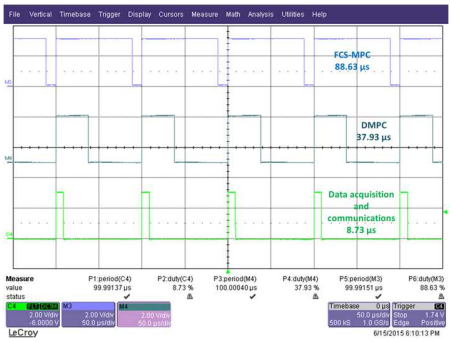

Fig. 9- Execution time for classical FCS-MPC, DMPC and Data communications only.

Experimental results under no-load condition are shown in Fig. 9, while Fig. 10 shows the obtained results when an active power flow of 4kW from port 1 to port 2 is demanded. In both cases DMPC is able to maintain the controlled variables at the desired reference values without noticeable steady state errors. A 4 kVAR step change of reactive power flow is shown in Fig. 11. The active power flow is completely unaffected by the

change in reactive power flow direction; phase currents immediately change according to the demanded reactive power flow. In Fig. 12 increased current distortion are present with respect to the obtained results in Fig. 11. This is mainly due to the different load conditions and to the fact that the DMPC resulting switching frequency is, as for any finite control set predictive control technique, variable. In Fig. 13 an 8 kW variation of the demanded active power flow with a slope of 1.5 kW/s is shown; in this case, DMPC is able to maintain accurate tracking during the duration of the active power transient.

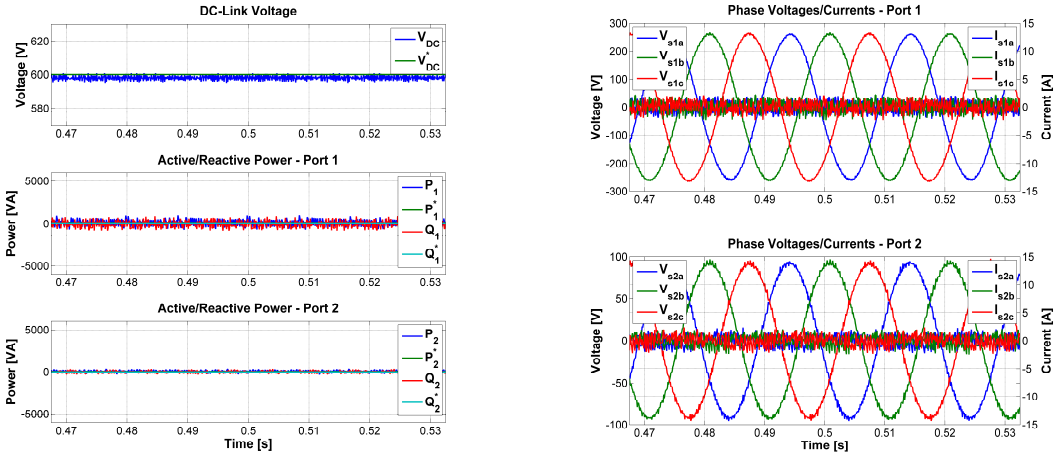

Fig. 10- Experimental results – DC-Link voltage, active/reactive powers, phase voltages and currents at both grid sides under no load conditions.

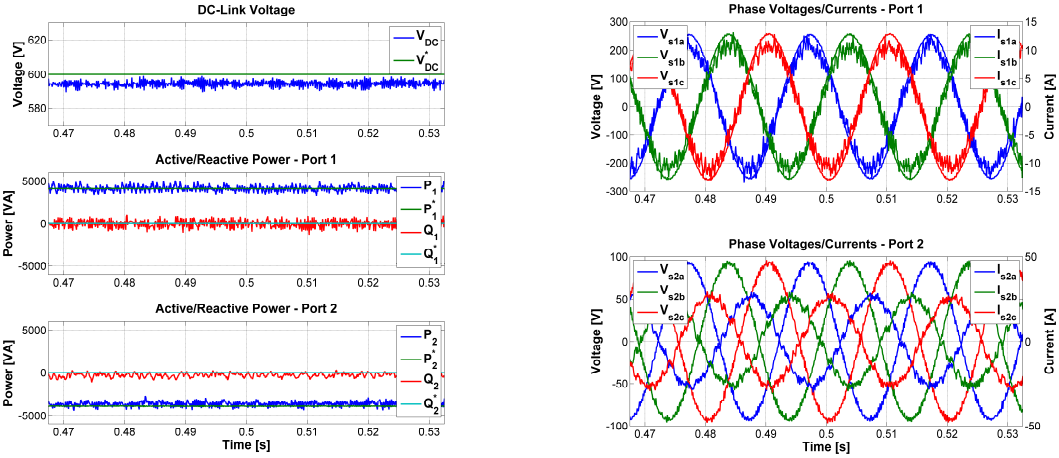

Fig. 11- Experimental results – DC-Link voltage, active/reactive powers, phase voltages and currents at both grid sides during a continuous 4kW active power flow from port 1 to port 2.

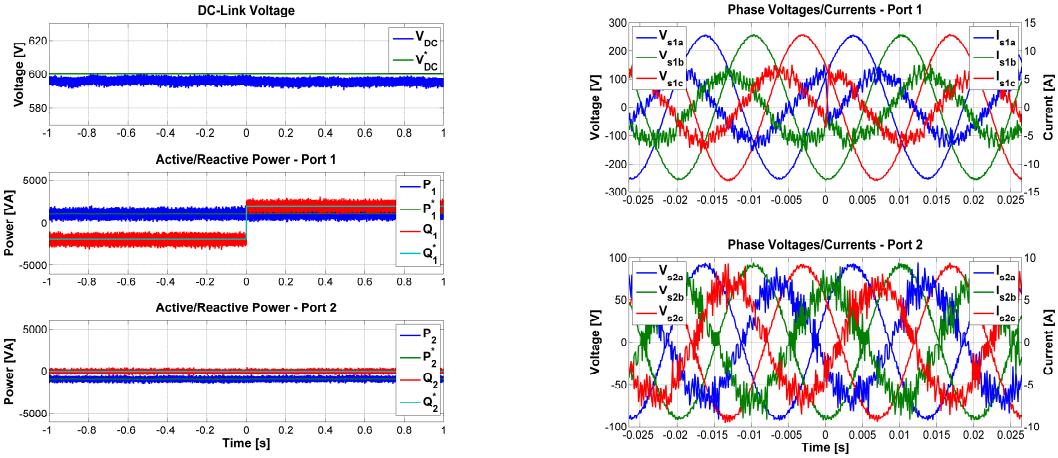

Fig. 12- Experimental results - DC-Link voltage, active/reactive powers, phase voltages and currents at both grid sides during a reactive power flow inversion of ±2kVAR while maintaining 1kW active power flow from port 1 to port 2.

Robustness to disturbances on the grid has been verified by introducing a 10 Hz frequency change and a 0.4 s long, 100% voltage dip at both grid sides as shown in Fig. 14 and Fig. 15, respectively. The frequency change (highlighted by the magenta line in Fig. 14) has negligible effects on the converter operation thanks to the fast response of DMPC and the absence of Phase Locked Loop in the controller implementation. During the voltage dip, the demanded active power grows as a consequence of the DC-Link discharge. Both ports try to reduce the DC-Link voltage discharge and normal operation are quickly restored after the voltage dip.

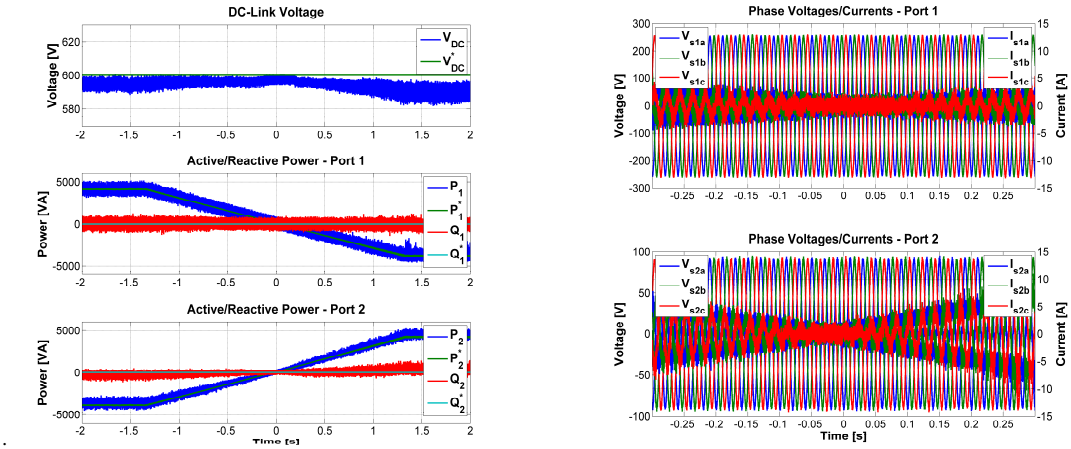

Fig. 13- Experimental results - DC-Link voltage, active/reactive powers, phase voltages and currents at both grid sides during an active power flow inversion ±4kW while maintaining 0kVAR of reactive power in both ports.

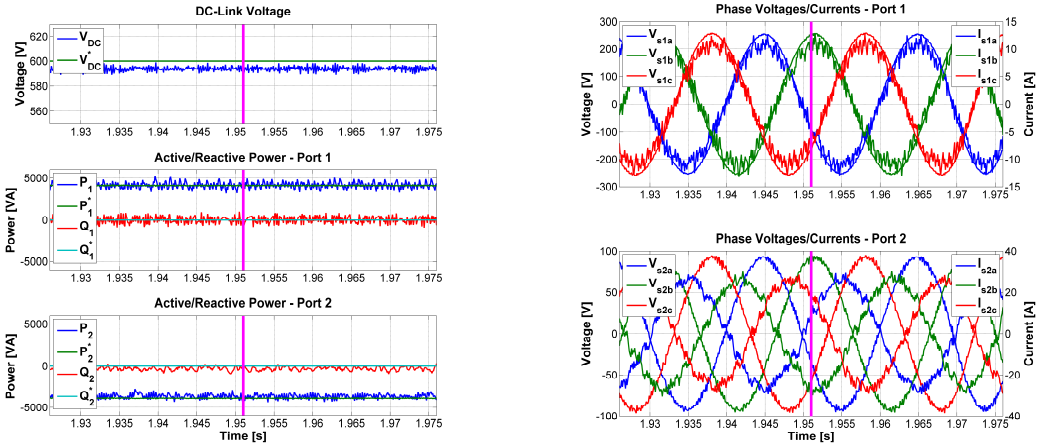

Fig. 14- Experimental results – DC-Link voltage, active/reactive powers, phase voltages and currents at both grid sides before and after a step change 50/60 Hz of the grid frequency.

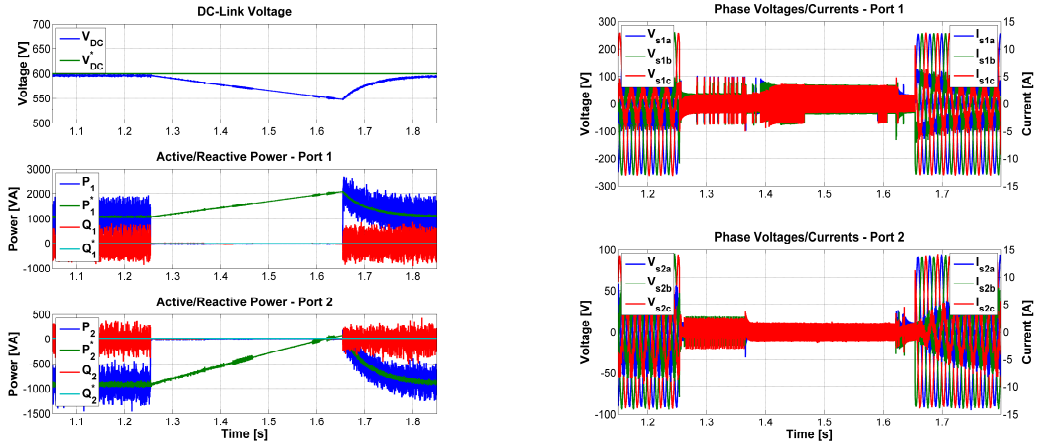

Fig. 15- Experimental results – DC-Link voltage, active/reactive powers, phase voltages and currents before, during and after a 0.4s long simultaneous 100% voltage dip at both grid sides.

V. Conclusions

In this paper, a distributed model predictive control strategy was proposed for the control of back-to-back converters. This control strategy was selected because it allows reducing the computational burden of predictive controllers, which is a widely recognized issue of these controllers in power electronics applications. Simulation and experimental tests were performed to evaluate the performance of the proposed control strategy. In both cases the control objectives were adequately satisfied despite the changes in the operating conditions of the converter and of the grid. Power flow has been successfully controlled while keeping voltage and current waveform of both converters regulated at the desired values and with high power quality, as well as the voltage at the DC-Link.

References

[1] S. Li, Z. Y, and Z. Q, "Nash-optimization enhanced distributed model predictive control applied to the Shell benchmark problem," *Inf. Sci. (Ny).*, vol. 170, no. 4, pp. 329–349, 2005.

[2] H. a. Young, M. a. Perez, J. Rodriguez, and H. Abu-Rub, "Assessing finite-control-set model predictive control: A comparison with a linear current controller in two-level voltage source inverters," *IEEE Ind. Electron. Mag.*, vol. 8, no. March, pp. 44–52, 2014.

[3] F. Di Palma and L. Magni, "A multi-model structure for model predictive control," *Annu. Rev. Control*, vol. 28, no. 1, pp. 47–52, 2004.

[4] W. Dumbar and S. Desa, "Distributed MPC for dynamic supply chain management," in *Assessment and Future Directions of Nonlinear Model Predictive Control*, 2007, pp. 607–615.

[5] I. Necoara, D. Doan, and A. K. Suykens, "Application of the proximal center decomposition method to distributed model predictive control," in *IEEE Conference on Decision and Control*, 2008.

[6] J. Rodríguez and M. P. Kazmierkowski, "State of the Art of Finite Control Set Model Predictive Control in Power Electronics," *IEEE Trans. Ind. Informat.*, vol. 9, no. 2, pp. 1003–1016, 2013.

[7] S. Kouro, P. Cortés, R. Vargas, U. Ammann, and J. Rodríguez, "Model predictive control—A simple and powerful method to control power converters," *IEEE Trans. Ind. Electron.*, vol. 56, no. 6, pp. 1826–1838, 2009.

[8] T. Geyer, N. Oikonomou, G. Papafotiou, and F. D. Kieferndorf, "Model Predictive Pulse Pattern Control," *IEEE Trans. Ind. Appl.*, vol. 48, no. 2, pp. 663–676, 2012.

[9] L. Tarisciotti, P. Zanchetta, A. Watson, J. C. Clare, S. Member, M. Degano, and S. Bifaretti, "Modulated Model Predictive Control for a Three-Phase Active Rectifier," *IEEE Trans. Ind. Appl.*, vol. 51, no. 2, pp. 1610–1620, 2015.

[10] S. Vazquez, J. I. Leon, L. G. Franquelo, J. Rodrigues, H. A. Young, A. Marquez, and P. Zanchetta, "Model predictive control: A review of its applications in power electronics," *IEEE Ind. Electron. Mag.*, vol. 8, no. 1, pp. 16–31, 2014.

[11] P. Karamanakos, T. Geyer, N. Oikonomou, F. D. Kieferndorf, and S. Manias, "Direct model predictive control: A review of strategies that achieve long prediction intervals for power electronics," *IEEE Ind. Electron. Mag.*, vol. 8, no. 1, pp. 32–43, 2014.

[12] P. Cortés, M. P. Kazmierkowski, R. M. Kennel, D. E. Quevedo, and J. Rodríguez, "Predictive Control in Power Electronics and Drives," *IEEE Trans. Ind. Electron.*, vol. 55, no. 12, pp. 4312–4324, 2008.

[13] S. Thomsen, "PI control, PI-based state space control, and model-based predictive control for drive systems with elastically coupled loads—A comparative study," *IEEE Trans. Ind. Electron.*, vol. 58, no. 8, pp. 3647–3657, 2011.

[14] L. Tarisciotti, P. Zanchetta, A. Watson, J. Clare, and S. Bifaretti, "Improving power quality with multi-objective Modulated Model Predictive Control," in *IEEE Energy Conversion Congress and Exposition (ECCE)*, 2014, pp. 5029–5036.

[15] R. P. Aguilera, P. Lezana, and D. E. Quevedo, "Finite-Control-Set Model Predictive Control With Improved Steady-State Performance," *IEEE Trans. Ind. Informat.*, vol. 9, no. 2, pp. 658–667, May 2013.

[16] J. Barros, F. Silva, and E. Jesus, "Fast predictive optimal control of NPC multilevel converters," *IEEE Trans. Ind. Electron.*, vol. 60, no. 2, pp. 619–627, 2013.

[17] J. Barros and F. Silva, "Optimal Predictive Control of Three-Phase NPC Multilevel Converter for Power Quality Applications," *IEEE Trans. Ind. Electron.*, vol. 55, no. 10, pp. 3670–3681, 2008.

[18] L. Tarisciotti, P. Zanchetta, A. J. Watson, J. C. Clare, and S. Bifaretti, "A comparison between Dead-Beat and Predictive control for a 7-Level Back-To-Back Cascaded H-Bridge under fault conditions," in *IEEE Energy Conversion Congress and Exposition (ECCE)*, 2013, pp. 2147–2154.

[19] L. Tarisciotti, P. Zanchetta, A. Watson, J. Clare, and S. Bifaretti, "Modulated Model Predictive Control for a 7-Level Cascaded H-Bridge back-to-back Converter," *IEEE Trans. Ind. Electron.*, vol. 61, no. 10, pp. 5375 – 5383, 2014.

[20] P. Cortés, A. Wilson, S. Kouro, J. Rodríguez, and H. Abu-Rub, "Model predictive control of multilevel cascaded H-bridge inverters," *IEEE Trans. Ind. Electron.*, vol. 57, no. 8, pp. 2691–2699, 2010.

[21] R. Vargas, J. Rodríguez, U. Ammann, and P. W. Wheeler, "Predictive Current Control of an Induction Machine Fed by a Matrix Converter With Reactive Power Control," *IEEE Trans. Ind. Electron.*, vol. 55, no. 12, pp. 4362–4371, 2008.

[22] E. Camponogara, D. Jia, B. H. Krogh, and S. Talukdar, "Distributed Model Predictive Control," *IEEE Control Syst. Mag.*, vol. 37, no. 5, pp. 732–745, 2007.

[23] E. Camponogara and S. Talukdar, "Distributed model predictive control: Synchronous and asynchronous computation," *IEEE Trans. Syst. Man, Cybern. Part A*, vol. 32, no. 5, pp. 732–745, 2007.

[24] M. D. Doan, T. Keviczky, and B. De Schutter, "An iterative scheme for distributed model predictive control using fenchel's duality," *J. Process Control*, vol. 21, no. 5, pp. 746–755, 2011.

[25] R. R. Negenborn, B. De Schutter, and J. Hellendoorn, "Multi-agent model predictive control for transportation networks: Serial versus parallel schemes," *Eng. Appl. Artif. Intell.*, vol. 21, no. 3, pp. 353–366, 2008.

[26] I. Alvarado, D. Limon, D. Muñoz de la Peña, J. M. Maestre, M. A. Ridao, H. Scheu, W. Marquardt, R. R. Negenborn, B. De Schutter, F. Valencia, and J. Espinosa, "A comparative analysis of distributed MPC techniques applied to the HD-MPC four-tank benchmark," , vol. 21, no. 5, pp. ," *J. Process Control*, vol. 21, no. 5, pp. 800–815, 2011.

[27] X. Du, Y. Xi, and S. Li, "Distributed model predictive control for large-scale systems," in *Proceedings of the 2001 American Control Conference, Arlington*, 2001.

[28] F. Y. Wang and I. T. Cameron, "A multi-form modelling approach to the dynamics and control of drum granulation processes," , vol. 179, no. 1-2, pp. , 2007," *Powder Technol.*, vol. 179, no. 1–2, pp. 2–11, 2007.

[29] J. Pimentel and M. Salazar, "Dependability of distributed control system fault tolerant units," in *28th Annual Conference of the IEEE Industrial Electronics Society (IECON)*, 2002.

[30] S. Talukdar, D. Jia, P. Hines, and B. H. Krogh, "Distributed model predictive control for the mitigation of cascading failures," in *Proceedings of the 44th IEEE Conference on Decision and Control and the 2005 European Control Conference*, 2005.

[31] A. H. Yang, X. Chen, and J. L. Alty, "Design issues and implementation of Internet-based process control systems," *Control Eng. Pactice*, vol. 11, no. 6, pp. 709–720, 2003.

[32] H. Zhao, Q. Wu, Q. Guo, H. Sun, and Y. Xue, "Distributed Model Predictive Control of a Wind Farm for Optimal Active Power Control&amp - Part II: Implementation With Clustering-Based Piece-Wise Affine Wind Turbine Model," *IEEE Trans. Sustain. Energy*, vol. 6, no. 3, pp. 1–10, 2015.

[33] H. Zhao, Q. Wu, Q. Guo, H. Sun, and Y. Xue, "Distributed Model Predictive Control of a Wind Farm for Optimal Active Power Control&amp - Part I: Clustering-Based Wind Turbine Model Linearization," *IEEE Trans. Sustain. Energy*, vol. 6, no. 3, pp. 1–10, 2015.

[34] Y. Wang, Z. Chen, X. Wang, Y. Tian, Y. Tan, and C. Yang, "An Estimator-Based Distributed Voltage-Predictive Control Strategy for AC Islanded Microgrids," *IEEE Trans. Power Electron.*, vol. 30, no. 7, pp. 3934–3951, 2015.

[35] M. Moradzadeh and R. Boel, "Voltage coordination in multi-area power systems via distributed model predictive control," *IEEE Trans. Power Syst.*, vol. 28, no. 1, pp. 513–521, 2013.

[36] K. Meng, Z. Y. Dong, S. Member, Z. Xu, S. Member, and S. R. Weller, "Cooperation-Driven Distributed Model Predictive Control for Energy Storage Systems," *IEEE Trans. Smart Grid*, vol. 6, no. 1, pp. 1–3, 2015.

[37] J. Liu, X. Chen, D. Muñoz de la Peña, and P. D. Christofides, "Sequential and iterative architectures for distributed model predictive control of

nonlinear process systems. Part II: Application to a catalytic alkylation of benzene," *Am. Control Conf.*, vol. 1, pp. 3156–3161, 2010.
[38] J. Liu, X. Chen, D. M. Muñoz de la Pena, and P. D. Christofides, "Sequential and iterative architectures for distributed model predictive control of nonlinear process systems. Part I: Theory," *Am. Control Conf.*, pp. 3148–3155, 2010.
[39] J. Liu, X. Chen, D. M. De La Peña, and P. D. Christofides, "Iterative distributed model predictive control of nonlinear systems: Handling asynchronous, delayed measurements," *IEEE Trans. Autom. Control*, vol. 57, no. 2, pp. 528–534, 2012.
[40] J. Liu, D. Muñoz de la Peña, and P. D. Christofides, "Distributed model predictive control of nonlinear systems subject to asynchronous and delayed measurements," *Automatica*, vol. 46, no. 1, pp. 52–61, 2010.
[41] C. Portilla, F. Valencia, J. D. López, J. Espinosa, A. Núñez, and B. De Schutter, "Non-linear model predictive control based on game theory for traffic control on highways," in *Proceedings of the 4th IFAC Nonlinear Model Predictive Control Conference*, 2012.
[42] F. Valencia, J. Espinosa, B. De Schutter, and K. Stanková, "Feasible-cooperation distributed model predictive control scheme based on game theory," in *Proceedings of the 18th IFAC World Congress*, 2011.
[43] F. Valencia, j. D. López, J. A. Patiño, and J. Espinosa, "Bargaining game based distributed model predictive control," in *Distributed Model Predictive Control Made Easy*, 2013, pp. 41–56.
[44] D. Jia and B. H. Krogh, "Distributed Model Predictive Control," in *American Control Conference, 2001. Proceedings of the 2001*, 2001.
[45] M. A. Perez, J. Rodríguez, E. J. Fuentes, and F. Kammerer, "Predictive Control of AC–AC Modular Multilevel Converters," *IEEE Trans. Ind. Electron.*, vol. 59, no. 7, pp. 2832–2839, Jul. 2012.
[46] J. Qin and M. Saeedifard, "Predictive control of a modular multilevel converter for a back-to-back HVDC system," *IEEE Trans. Power Del.*, vol. 27, no. 3, pp. 1538–1547, 2012.
[47] J. Bocker, B. Freudenberg, A. The, and S. Dieckerhoff, "Experimental Comparison of Model Predictive Control and Cascaded Control of the Modular Multilevel Converter," *IEEE Trans. Power Electron.*, vol. 30, no. 1, pp. 422–430, 2015.
[48] M. Vatani, B. Bahrani, M. Saeedifard, and M. Hovd, "Indirect Finite Control Set Model Predictive Control of Modular Multilevel Converters," *IEEE Trans. Smart Grid Sm*, vol. 6, no. 3, pp. 1520–1529, 2015.
[49] S. Bifaretti, P. Zanchetta, A. J. Watson, L. Tarisciotti, and J. C. Clare, "Advanced power electronic conversion and control system for universal and flexible power management," *IEEE Trans. Smart Grid*, vol. 2, no. 2, pp. 231–243, 2011.
[50] S. Bifaretti, P. Zanchetta, A. J. Watson, L. Tarisciotti, and J. C. Clare, "Predictive control for universal and flexible power management," in *IEEE Energy Conversion Congress and Exposition (ECCE)*, 2010, pp. 3847–3854.

Luca Tarisciotti (S'12-M'15) received the Master's degree in electronic engineering from The University of Rome "Tor Vergata" in 2009 and his Ph.D. degree in Electrical and Electronic Engineering from the PEMC group, University of Nottingham in 2015. He is currently working as Research Fellow at the University of Nottingham, UK. His research interests includes matrix converters, DC/DC converters, multilevel converters, advanced modulation schemes, and advanced power converter control.

Giovanni Lo Calzo received the Master's degree and the PhD degree from the University of ROMA TRE, Rome, Italy, respectively in 2010 and 2015. From 2010 to 2011, he was a Research Assistant with the University of Roma Tre. He is currently a Research Fellow with The University of Nottingham, Nottingham, UK, in the Power Electronics, Machine and Control Group. His research interests are mainly focused on power electronics converters for high speed machines, control and modelling of grid-tied and isolated inverters, output filter topologies.

Alberto Gaeta (S' 08) received the M.S. and Ph.D degrees in electrical engineering from the University of Catania, Catania, Italy, in 2008 and 2011, respectively. From 2013 to 2015 he joined the Power Electronics and Machine Control Group at the University of Nottingham. Currently he works as a consultant for several comnpanies. He is a member of the IEEE Industrial Electronics, IEEE Industry Applications, IEEE Power Electronics Societies. His research interests include power electronics and high performance drives, with particular attention to predictive, fault tolerant and sensorless control techniques.

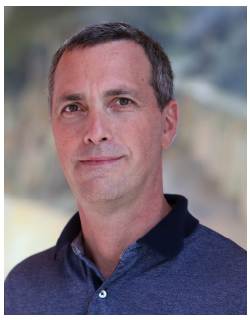

Pericle Zanchetta (M'00–SM'15) received his Master degree in Electronic Engineering and his Ph.D. in Electrical Engineering from the Technical University of Bari (Italy) in 1994 and 1998 respectively. In 1998 he became Assistant Professor of Power Electronics at the same University. In 2001 he became lecturer in control of power electronics systems in the PEMC research group at the University of Nottingham – UK, where he is now Professor in Control of Power Electronics systems. He has published over 220 peer reviewed papers; he is Chair of the IAS Industrial Power Converter Committee (IPCC) and associate editor for the IEEE transactions on Industry applications and IEEE Transaction on industrial informatics. He is member of the European Power Electronics (EPE) Executive Council. His general research interests are in the field of Power Electronics, Power Quality, Renewable energy systems and Control.

Felipe Valencia (M'13) was born in Medellín, Colombia. He received the Master's and Ph.D. (magna cum laude) degrees in control engineering from the Univeridad Nacional de Colombia, Medellín. He is a Control Engineer with the Universidad Nacional de Colombia. He is currently a Full Time Researcher with the Solar Energy Research Center Solar Energy Research Centre-Chile, Department of Electrical Engineering, University of Chile, Santiago. His current research interests include design of distributed and hierarchical strategies for controlling large-scale systems, researching on different fields such as power energy generation, transmission, and distribution systems, transportation, and smartgrids.

Doris Sáez (S'93–M'96–SM'05) was born in Panguipulli, Chile. She received the M.Sc. and Ph.D. degrees in electrical engineering from the Pontificia Universidad Católica de Chile, Santiago, in 1995 and 2000, respectively. She is currently an Associate Professor with the Department of Electrical Engineering, University of Chile, Santiago. Her current research interests include predictive control, fuzzy control design, fuzzy identification, control of power generation plants, and control of transport systems. She has co-authored the books Hybrid Predictive Control for Dynamic Transport Problems (Springer-Verlag, 2013) and Optimization of Industrial Processes at Supervisory Level: Application to Control of Thermal Power Plants (Springer-Verlag, 2002). Dr. Sáez is an Associate Editor of the IEEE TRANSACTIONS ON FUZZY SYSTEMS.